

High-Temperature Oxidation Behavior of Al-Cr-Y Coating on Ni-based Superalloy Prepared by Pack Cementation

Cao Jiangdong¹, Tong Fuli²

¹ Nantong Shipping College, Nantong 226010, China; ² Jiangsu University, Zhenjiang 212003, China

Abstract: The oxidation behaviors of Al-Cr-Y coatings with different Al contents prepared by pack cementation process were investigated. The results show that the coating with 2 wt% Al in the pack has a three-layer structure, while the coatings with 2.5 wt% and 3 wt% Al have two layers. In addition, the main phases in the coatings with 2 wt% and 3 wt% Al are α -Cr and NiAl, respectively, while the main phase in the coating with 2.5 wt% Al is NiAl with several Cr-rich particles and solid-solution Cr atoms in the coating. The oxidation test demonstrates that the coated specimen with 2 wt% Al has the poorest oxidation resistance and the coated specimen with 2.5 wt% Al has the best oxidation resistance.

Key words: superalloy; oxidation; surface; coating

Ni-based superalloys are primarily designed for applications in aerospace and industrial gas turbines because of their excellent mechanical properties at high temperature. However, Ni-based superalloys also serve in extreme oxidizing environments, and degradation caused by high-temperature oxidation restricts their efficiency in industrial gas turbines^[1]. In these environments, adding a coating is an effective way to protect components. Aluminide diffusion coatings are conventional coatings designed and developed to provide oxidation protection for Ni-based superalloys in extremely harsh environments^[2, 3]. In an aggressive environment, a compact and well-adhered oxide layer is formed, helping prevent both the inward diffusion of oxygen and the outward diffusion of matrix elements, such as Ni and Ti^[4]. However, with increasing the working temperatures of superalloys, conventional aluminide coatings cannot provide adequate oxidation protection^[5].

In the past several decades, several studies have revealed that with sufficient control of pack chemistry and codeposition conditions, chromium, silicon, lanthanum, and cobalt aluminizing coatings can be prepared to significantly enhance oxidation resistance of superalloys^[4, 6-9]. Also, a series of investigations have been performed about chromium-aluminizing coatings by Coasta and Lu^[10, 11]. Furthermore, Xiang^[9] and Wu^[12]

et al have examined chromium-aluminizing coatings on Ni-based superalloys and discussed the subsequent pack thermodynamics. Different categories of activators and pack powder compositions have also been studied, indicating that coatings usually have a complex structure consisting of three or four major distinctive layers, and the structure is determined by the pack composition and process parameters. For example, adding small quantities of Y has a positive effect on oxidation resistance and reduces oxide scale spallation from coating surfaces^[3, 5, 13, 14]. However, the microstructure and oxidation resistance of yttrium-chromium-aluminizing coatings have seldom been studied.

While many methods can be employed to prepare diffusion coatings, pack cementation is an effective and economic method that can produce uniform and smooth diffusion coatings with suitable thicknesses on components with complicated shapes. In this work, yttrium-chromium-aluminizing coatings with different Al contents were prepared on the Ni-based superalloy GH586 by a halide-activated pack cementation process. The phase composition and microstructure of all coatings before and after oxidation were studied. Afterwards, the growth mechanisms of coatings produced by pack cementation were discussed. In addition, the oxidation degra-

Received date: November 24, 2018

Foundation item: Natural Science Foundation of Jiangsu Province (16KJB430035); Qing Lan Project of Jiangsu Province

Corresponding author: Cao Jiangdong, Ph. D., Associate Professor, Mechanical and Electrical Department, Nantong Shipping College, Nantong 226010, P. R. China, Tel: 0086-513-85965515, E-mail: caojd@ntsc.edu.cn

Copyright © 2019, Northwest Institute for Nonferrous Metal Research. Published by Science Press. All rights reserved.

dation mechanism of yttrium-chromium-aluminizing coatings and the beneficial effects of Cr in coatings were also discussed.

1 Experiment

The substrate of the coated specimens was a GH586 superalloy with nominal composition shown in Table 1, and the specimens were standard heat treated and mainly composed of the γ matrix and the γ' phase [15]. The specimens were cut to dimensions of approximately 10 mm×10 mm×5 mm by electro-discharge machining and manually ground with abrasive paper to a 1500 grit finish. Then, the specimens were further polished, ultrasonically degreased, and cleaned in acetone before the pack cementation process.

The pack powder mixture was prepared by mixing appropriate proportions of Cr, Al, Y_2O_3 , NH_4Cl , and Al_2O_3 powders, and the average particle sizes of these powders were <100 mesh. Based on previous investigations [3, 5, 16, 17], three pack mixtures containing 2 wt%, 2.5 wt%, and 3 wt% Al (Table 2) were designed. The superalloy specimens were then buried into pack powders and placed into an alumina crucible, which was sealed with an alumina lid and cement. Fig.1 shows a schematic diagram of the pack cementation process. Under an argon gas flow, the retort was heated to 1113 K at a rate of 7 K·min⁻¹, and held at this temperature for 8 h. Then, the alumina tube furnace and crucible were gradually cooled to room temperature.

Oxidation tests were performed to evaluate the protective effect of the coatings. First, coated specimens were cleaned and then placed in an alumina crucible, and all the samples were placed into the crucibles and kept in line contact with crucible walls. After oxidation at 1273 K for 1, 3, 5, 10, 20, 40, 60, 80, and 100 h, the samples were weighed using an electronic balance with a sensitivity of 10⁻⁴ g, and the weight gain per unit area was calculated over various time periods.

The surface and cross-sectional morphologies of coated specimens before and after oxidation were observed by scanning electron microscopy (SEM; JSM-7001F, JEOL Ltd, Tokyo, Japan), and elemental composition was analyzed by energy dispersive spectroscopy (EDS). In addition, X-ray dif-

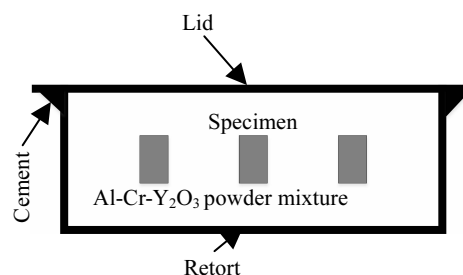


Fig.1 Schematic diagram of pack cementation process

fraction (XRD, Cu K α) with a 2θ range of 10°~90° was employed to investigate surface phase structures before and after oxidation.

2. Results and Discussion

2.1 Coating characterization

XRD patterns in Fig.2 show the phases in the Al-Cr-Y coatings with different Al pack contents. It can be seen that the main phases in the coating with 2 wt% Al are α -Cr, Ni₃Al, and a small amount of Al_2O_3 , in which α -Cr was observed in previous studies of diffusion aluminides doped with chromium and reactive elements [9, 18, 19]. In contrast, the patterns of the coatings with 2.5 wt% and 3wt% Al show that the main phase of the coatings is β -NiAl. All the coatings have a small quantity of Al_2O_3 , indicating that there is an outward diffusion of Ni [9, 20].

Fig.3a shows the cross-sectional SEM image of specimen with the pack content of 2 wt% Al, and that the coating possesses a three-layer structure composed of an outer layer, an inner layer, and a diffusion zone. The outer layer is about 3 μ m thick, while the inner layer of 2 μ m contains homogeneously distributed pores. The pores form in the coating because several kinds of atoms moving at different diffusion rates form hollowed areas, which is called the Kirkendall effect [21-23]. The diffusion zone is about 5 μ m thick beneath the inner layer, suggesting that the coating formation is primarily attributed to outward Ni diffusion [21]. The major elemental concentrations of the coatings measured by EDS show that the outer layer composition is 43Cr-23Ni-20Al-10Co-0.5Y and the inner layer is 62Cr-26Ni-10Al-10Co (at%, Fig.3b). Y is only detected in the outer layer of coating, which is similar to previous research by Pang [23], while Cr is the dominant element in the outer and inner layers. Combined with the XRD results, the main phase in the outer and inner layers is α -Cr [18]. However, limited Al is deposited in these layers when Cr deposition occurs.

Cross-sectional SEM image of specimen with 2.5 wt% Al shows that unlike the specimen with 2 wt% Al, this coating only consists of an outer layer and a diffusion zone with thicknesses of 20 and 10 μ m, respectively (Fig.4a). Also, the elemental composition of the coating measured by EDS shows that the outer layer is mainly composed of light particles distributed in the coating, which are Cr-rich and Al-rich

Table 1 Nominal composition of GH586 superalloy (wt%)

Al	Ti	Mo	Cr	W	Co	C	Ni
1.6	3.2	8	19	3	11	0.06	Bal.

Table 2 Composition of three Al-Cr-Y powder mixtures (wt%)

Al	Y_2O_3	Cr	NH_4Cl	Al_2O_3
2	4	20	4	70
2.5	4	20	4	69.5
3	4	20	4	69

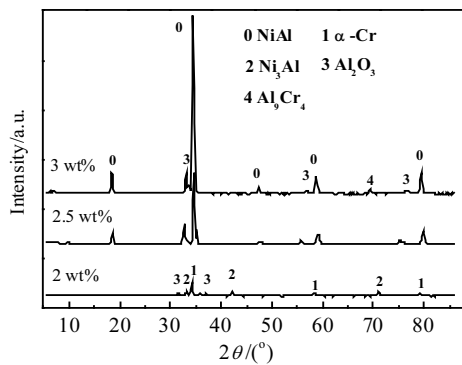


Fig.2 XRD patterns of surface of the coated specimens with different Al contents

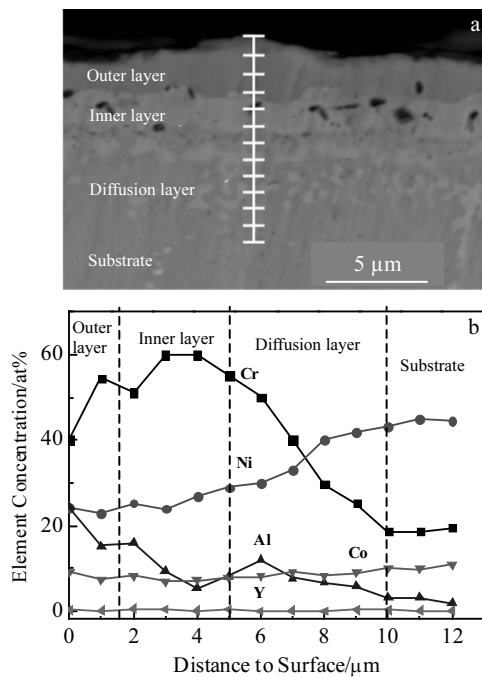


Fig.3 Cross-sectional SEM image (a) and major element concentration profiles (b) of specimen with 2 wt% Al

phases (Fig.4b). In contrast, the elemental composition of the light particles, such as point 0 in the magnified zone of Fig.4a, is 26.49Al-0.89Ti-47.72Cr-2.32Co-6.00Mo-1.54W-15.03Ni (at%), while the matrix is 38.75Al-0.43Y-1.40Cr-7.98Co-1.10Ti-49.84Ni (at%). Combined with the XRD data, the light particles mainly contain the Al_9Cr_4 phase.

By increasing the Al content to 3 wt%, the formed coating has a thickness about 20 μm and a two-layer structure with an outer layer and a diffusion zone (Fig.5a), whose thicknesses are 12 and 8 μm , respectively. Also, high magnification observations of the cross-sectional microstructure in Fig.5a show that light particles are uniformly distributed in the dark matrix. Furthermore, EDS analysis reveals that the light particles possess elemental composition similar to the dark matrix.

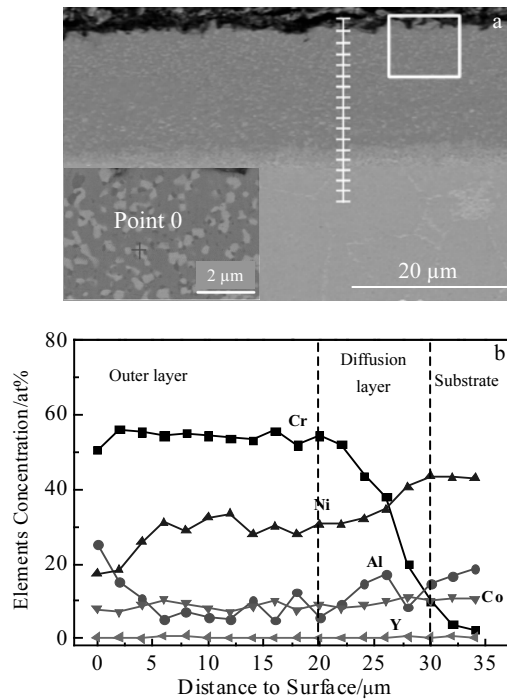


Fig.4 Cross-sectional SEM image (a) and major element concentration profiles (b) of specimen with 2.5 wt% Al

Specifically, the elemental composition of the light particles and the dark matrix are 34.36Al-0.42Y-3.16Cr-10.54Co-5.56Mo-46.94Ni (at%) and 39.25Al-0.33Y-1.30Cr-6.98Co-1.05Mo-50.89Ni (at%), respectively.

2.2 High-temperature oxidation resistance

The high-temperature oxidation resistance of the coated specimens and the substrate, evaluated by the time-related mass changes with heating at 1273 K, shows that the mass change rate of the substrate increases quickly at the beginning of the oxidation and then decreases to a constant rate of 2.60 mg/cm^2 (Fig.6). In the early stages of oxidation (10 h), the mass of the specimens with 2 wt% Al increases quickly in the initial 5 h, and then rapidly decreases. Nonetheless, after 100 h, the specimen is almost entirely oxidized. The specimens with 3 wt% Al exhibit better oxidation resistance, whose mass-gain curve follows a parabolic law, reaching 1.20 mg/cm^2 after 100 h of oxidation. From the mass gain curves in Fig.6, specimens with 2.5 wt% Al exhibit the best oxidation resistance, reaching 0.85 mg/cm^2 after 100 h of oxidation.

XRD patterns (Fig.7) of the surfaces of all coated specimens after oxidation at 1273 K for 100 h show that the surface oxides of specimen with 2 wt% Al are mainly composed of Cr_2O_3 , NiCr_2O_4 , NiO as well as small quantities of TiO_2 . In other two specimens, Al_2O_3 is the major surface oxide phase, and small percentages of Cr_2O_3 , NiCr_2O_4 , and TiO_2 are also detected.

The surface morphologies and cross-sectional microstructures of all coated specimens after oxidation at 1273 K for 100 h

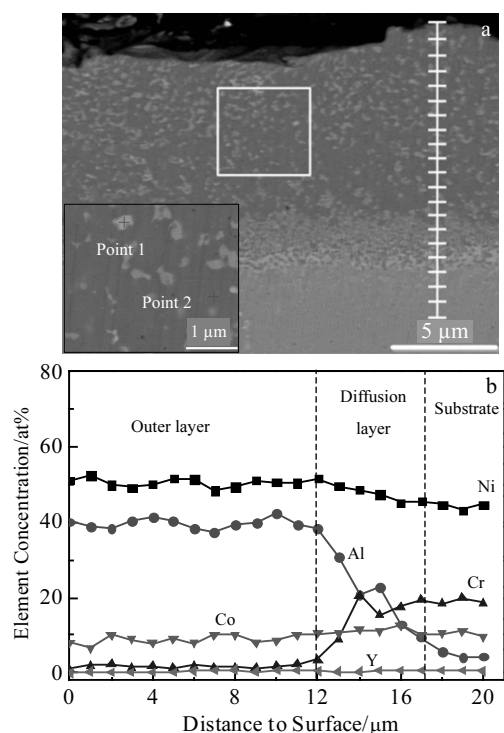


Fig.5 Cross-sectional SEM image (a) and major element concentration profiles (b) of specimen with 3 wt% Al

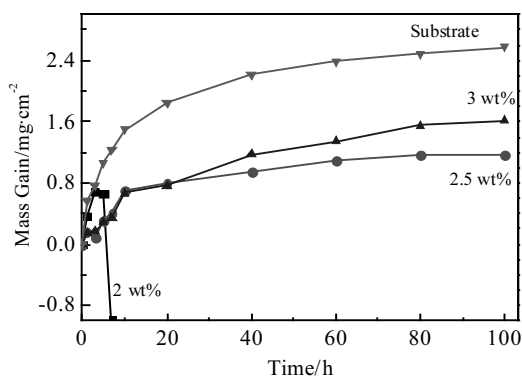


Fig.6 Mass change curves for the specimens with different Al contents at 1273 K for 100 h

show that spallation occurs in specimen with 2 wt% Al (Fig.8a). A high proportion of oxides, such as NiO, NiCr₂O₄, and Cr₂O₃, were determined from XRD and EDS data. The internal oxidation that occurs under the oxide scale of specimens with 2 wt% Al also indicates that the oxide scale does not provide adequate protection for the specimen (Fig.8b), which is in agreement with Pint and Liu's research^[12, 14, 24]. EDS analysis indicates that the oxide scale consists of 62.72 at% O, 7.28 at% Ni, 6.10 at% Ti, and 23.90 at% Cr, indicating that the oxides are probably Cr₂O₃, NiCr₂O₄, and TiO₂.

In contrast, compact and continuous Al₂O₃ scales are formed on surfaces of specimens with 2.5 wt% Al pack. In

addition, some granular oxides consisting of MoO₃ are non-uniformly distributed above the oxide scale in the samples (Fig.8c), and the oxide scale thickness is 15 μm (Fig.8d). EDS analysis demonstrates that the oxide scale mostly contains O (62.28 at%), Al (33.18 at%) and Ti (2.28 at%), indicating that the scale is in the form of Al₂O₃ with trace TiO₂. Also, the interface between the oxide scale and coating is not smooth, which improves adhesion^[3, 5]. The nature of the coating beneath the oxide scale is probably Ni₃Al and mainly composed of Al, Ni, and Co (21.18 at%, 68.28 at%, and 10.10 at%, respectively).

In specimens with 3 wt% Al, some rod-like oxides are observed on the surface, and they are determined to be TiO₂ (Fig.8e). Also, mixed oxides containing O, Al, Ti, and Cr (63.37 at%, 12.80 at%, 13.11 at%, and 11.03 at%, respectively) are detected above the oxide scale. The thickness of the specimens with 3 wt% Al is almost equal to that of the specimens with 2.5 wt% Al, reaching 15 μm (Fig.8f), and pores are also observed on the surface of the surfaces, indicating poor oxide scale adhesion. However, the oxide scale of the specimens with 3 wt% Al is probably Al₂O₃ and a small amount of TiO₂ and NiCr₂O₄, and the oxide scale contains O, Al, Cr, and Ti (59.80 at%, 32.10 at%, 4.62 at%, and 4.10 at%, respectively). In addition, the coating beneath the oxide scale is probably Ni₃Al and is mainly composed of Al, Ni, Co, and O (21.18 at%, 68.28 at%, 10.10 at%, and 5.25 at%, respectively), indicating that oxygen atoms penetrate deeply into the coating.

2.3 Discussion of formation mechanism and high temperature oxidation behavior of the coatings

2.3.1 Formation mechanism of the Y-Cr-Al coating

During the process of forming a coating by cementation pack, first NH₄Cl was decomposed into NH₃ and HCl (reaction (1)) at high temperature. Then, the resultant HCl reacted with Al, Cr and Y₂O₃ in the pack (reactions (2), (3), and (6)), generating CrCl₃, AlCl₃, and YCl₃. Subsequently, CrCl₃, AlCl₃, and YCl₃ were decomposed into atoms Al, Cr, and Y (reactions (4), (5), and (7)), and Y further reacted with CrCl₃ and AlCl₃ to form more Al and Cr atoms (reactions (8) and (9)). Thus, adding Y is beneficial for forming the Y-Cr-Al coating.

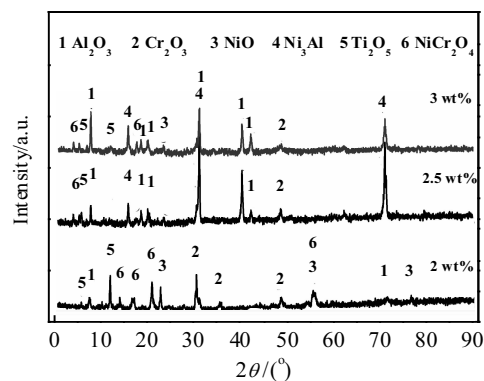


Fig.7 XRD patterns of surface of specimens with different Al contents after oxidation at 1273 K for 100 h

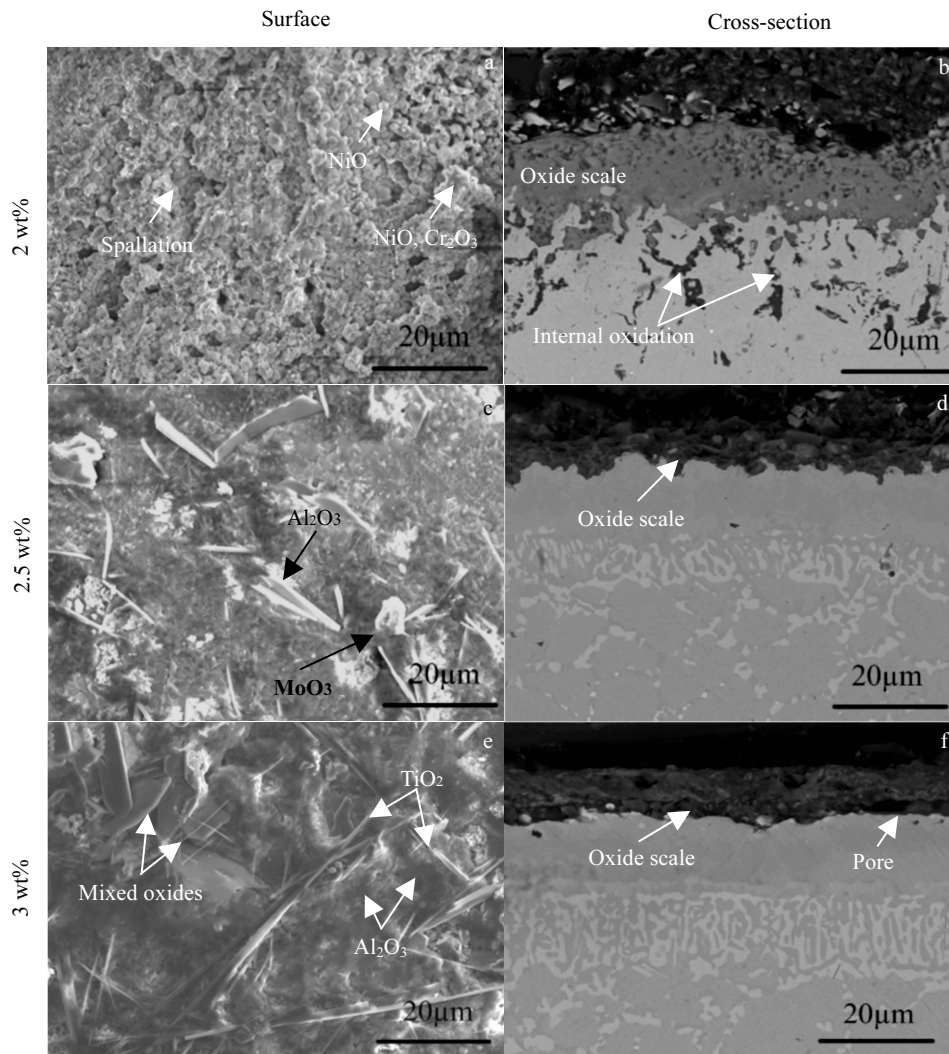


Fig.8 Morphologies (a, c, e) and microstructures (b, d, f) of all the specimens after oxidation at 1273 K for 100 h



Coating thicknesses increases with increasing the pack Al content. A small quantity of Y element was observed to be finely dispersed in the outer and inner layers, and according to Ref.[14, 23], these native active atoms, such as Cr^{3+} and Al^{3+} diffuse more quickly than Y atoms, which reduces the outward short-circuit transport of cations along the scale grain boundaries^[23, 25]. In the initial stage of the coating deposition process with 2 wt% Al pack content, Cr deposition dominates^[17] and only small concentrations of Al and Y atoms

(in Fig.9a) were deposited because the equilibrium partial pressure of CrCl_3 is much higher than that of AlCl_3 and YCl_3 . At a later stage, the equilibrium AlCl_3 partial pressure increased and more Al atoms were deposited in the coating, and then the deposited Al and Y atoms were dissolved in the α -Cr. Meanwhile, reactive elements, such as Ni, Co, and Mo, diffused outward from the substrate to the coating and reacted with the deposited elements. During this process, many pores formed in the coating due to the Kirkendall effect.

As the pack Al content increases to 2.5 wt%, codeposition of Al and Cr occurs because of the comparable equilibrium partial pressures of AlCl_3 and CrCl_3 around the specimen. It is observed that the outer layer are composed of Cr-rich and Al-rich phases. In Fig.9b, observations of coating structures suggest that codeposition of Al and Cr indeed occurs without the Kirkendall effect in the pack cementation process, and the coating is continuous and compact.

When the pack Al content increases to 3 wt%, the vapor

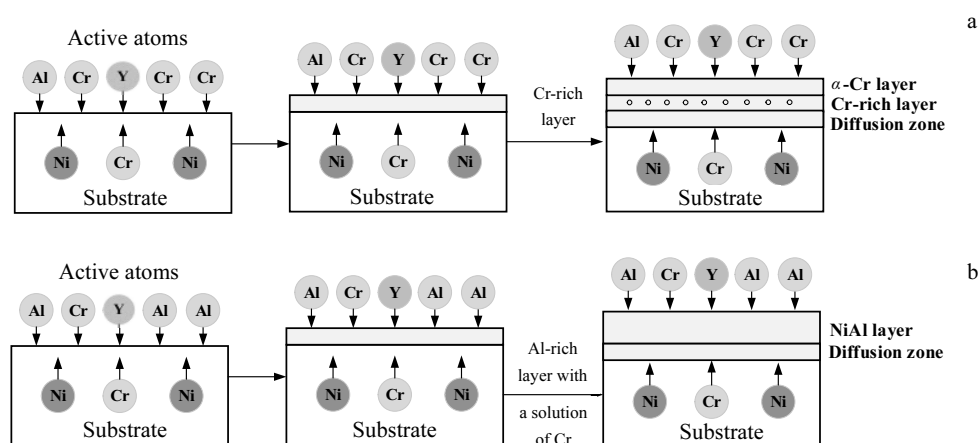


Fig.9 Schematic illustration of the packing process and the microstructure evolution of the coatings with different Al contents: (a) 2 wt%, and (b) 2.5 wt%

pressure of AlCl_3 becomes far higher than that of CrCl_3 , indicating that the deposition of Al atoms dominates in the process, increasing the coating thickness. At the same time, Ni and Cr atoms in the substrate diffuse outward to the coating and react with the deposition elements to form the phases of NiAl and Al_9Cr_4 .

2.3.2 Oxidation behavior of the coatings

In this study, the oxidation resistance of coated specimens fluctuates dramatically with pack Al content. The coating with 2 wt% Al content is thin and has many distributed pores, which negatively affect the formation of a continuous Cr_2O_3 scale and thus allow internal oxidation. At the same time, Ni and reactive elements, such as Ti and Mo, diffuse outward from the substrate metal to the gas interface, which increases spallation and coating oxidation^[25]. Moreover, as the oxidation continues, the Ni and Cr elements of the substrate diffusing to the surface encounter oxygen to form a few NiO and Cr_2O_3 on the surface. Because of the solid-state reaction $\text{NiO} + \text{Cr}_2\text{O}_3 \rightarrow \text{NiCr}_2\text{O}_4$, the resulting spinels formed on the surface also reduce oxidation resistance^[15].

As Al content increases to 2.5 wt%, continuous and compact oxide scales consisting mainly of Al_2O_3 form on specimen surfaces after oxidation. Then, due to the codeposition of Cr-Al-Y, the coating is rich in both Al and Cr, which contributes to the improvement of oxidation resistance^[24, 25]. At the beginning of oxidation, Cr and Ni atoms diffuse to the gas/coating surface interface to form Cr_2O_3 and NiO. However, Cr can react with NiO via the reaction $3\text{NiO} + 2\text{Cr} \rightarrow 3\text{Ni} + \text{Cr}_2\text{O}_3$. Thus, Cr_2O_3 scales form and eventually become continuous on the surface. Below this Cr_2O_3 scale, Al_2O_3 is developed as a metastable phase $\theta\text{-Al}_2\text{O}_3$. In long-term oxidation, Cr_2O_3 decomposes into CrO_3 and then evaporates, while $\theta\text{-Al}_2\text{O}_3$ becomes stable and is ultimately developed as a compact and continuous Al_2O_3 scale^[26, 27].

In addition, oxidation resistance decreases as the pack Al content increases to 3 wt%. In early oxidation, continuous and dense oxide scale did not develop and oxygen ions diffused inward through the grain boundary into the coating, leading to slight internal oxidation. Subsequently, the selective oxidation of coating occurred to form the continuous and compact Al_2O_3 scale on the coating surface, and there were other oxides (TiO_2 , Cr_2O_3 , NiO, etc.) in the oxidation film. These oxides on the Al_2O_3 scale may be caused by the diffusion of Ni, Ti and Cr ions along Al_2O_3 grain boundaries^[27]. The solid Y solution in the coating may increase oxidation resistance because Y atoms inhibit outward Ti ion migration along scale grain boundaries, thereby improving adhesion.

3 Conclusions

1) With increasing the pack Al content, coating microstructure changes greatly. The coating with 2 wt% Al content possesses a three-layer structure consisting of outer and inner layers and a diffusion zone. However, coatings with 2.5 wt% and 3 wt% Al content only consist of an outer layer and a diffusion zone without any pores.

2) There is a large difference in the main phases of the coatings with increasing the Al content. Coatings contains 2 wt% and 3 wt% Al pack possess clear Cr-rich and NiAl layers, respectively. For 2.5 wt% Al pack, Cr appears as a solid solution in the NiAl layer, which contains Cr-rich particles distributed homogeneously.

3) The coating with 2 wt% Al pack shows the poorest oxidation resistance due to the distributed pores and outward diffusion of Ni, Mo, and Ti. Also, the formation of spinels aggravates oxidation of the coating. However, the coating with 2.5 wt% Al pack demonstrates the best oxidation resistance because Cr and Y have positive effects that improve the resistance of high temperature oxidation.

References

- 1 Koo C H, Bai C Y, Luo Y J. *Mater Chem Phys*[J], 2004, 86(2-3): 258
- 2 Burigel R. *Metal Science Journal*[J], 1986, 2(3): 302
- 3 Zhao X, Zhou C. *Corros Sci*[J], 2014, 86: 223
- 4 Shirvani K, Saremi M. *Corros Sci*[J], 2003, 45(5): 1011
- 5 Liu Zongjie, Zhao Xiongsheng, Zhou Chungun. *Corros Sci*[J], 2015, 92: 148
- 6 Peng X, Li T, Pan W P. *Scripta Mater*[J], 2001, 44(7): 1033
- 7 Qiao Min, Zhou Chungun. *Corros Sci*[J], 2012, 206(11-12): 2899
- 8 Xiang Z D, Datta P K. *Sci Eng A*[J], 2003, 356(1-2): 136
- 9 Xiang Z D, Burnell-Gray J S, Datta P K. *Surf Eng*[J], 2001, 17(4): 287
- 10 Coasta W Da, Gleeson B, Young D J. *Surf Coat Tech*[J], 1997, 88(1-3): 165
- 11 Lu Jintao, Zhu Shenglong, Wang Fuhui. *Oxid Met*[J], 2011, 76(1-2): 67
- 12 Wu Duoli, Jiang Sumeng, Fang Qixiang et al. *Acta Metall Sin*[J], 2014, 27(4): 627
- 13 Rover F, Mayrhofer P H, Reinholdt A et al. *Surf Coat Tech*[J], 2008, 202(24): 5870
- 14 Pint B A, Haynes J A, Besmann T M. *Surf Coat Tech*[J], 2010, 204(20): 3287
- 15 Hua Yinqun, Rong Zhen, Ye Yunxia et al. *Appl Surf Sci*[J], 2015, 330: 439
- 16 Zhang Ping, Guo Xiping. *Corros Sci*[J], 2013, 71: 10
- 17 Rahman A, Chaula V, Jayaganthan R et al. *Mater Chem Phys*[J], 2011, 126(1-2): 253
- 18 Bestor M A, Alfano J P, Weaver M L. *Intermetallics*[J], 2011, 19(11): 1693
- 19 Robert Bianco, Robert A, Rapp J. *Electrochem Soc*[J], 1993, 140: 1181
- 20 Xiang Z D, Datta P K. *Surf Coat Tech*[J], 2004, 179(1): 95
- 21 Qiao Min, Zhou Chungun. *Corros Sci*[J], 2013, 75(11-12): 454
- 22 Garbala K, Patejuk A. *Archives of Foundry Engineering*[J], 2010, 10: 455
- 23 Pang Q, Wu G H, Sun D L et al. *Mater Sci Eng A*[J], 2013, 568: 228
- 24 Liu Zhenyu, Gao Wei. *Scripta Mater*[J], 1998, 38(6): 877
- 25 Pint B A. *Oxid Met*[J], 1996, 45(1-2): 1
- 26 Carl Wanger. *J Electrochem Soc*[J], 1956, 103 (11): 627
- 27 Prescote R, Graham M J. *Oxi Met*[J], 1992, 38(3-4): 233

粉末包埋法制备镍基高温合金 Al-Cr-Y 涂层的高温氧化行为

曹将栋¹, 童福利²

(1. 南通航运职业技术学院, 江苏 南通 226010)

(2. 江苏大学, 江苏 镇江 212003)

摘要: 为了提高高温合金的抗高温氧化性能, 采用粉末包埋法制备了镍基高温 Al-Cr-Y 涂层, 研究了不同 Al 含量涂层的高温氧化行为, 并通过 XRD, SEM 对涂层的物相和形貌进行了分析。结果表明: 含有 2% (质量分数) 的 Al 粉所制备的涂层呈 3 层结构, 主要相为 α -Cr, 而含有 2.5% 和 3% Al 粉的涂层为双层结构, 主要相为 NiAl, 在含有 2.5% Al 粉的涂层中存在富 Cr 的固溶体。经高温氧化实验看出, 含有 2% Al 粉涂层的抗高温氧化性能最差, 含 2.5% Al 粉的涂层在 1000 °C 下形成了致密连续的氧化膜, 起到了很好的保护作用, 表现出优异的抗高温氧化性能。

关键词: 高温合金; 高温氧化行为; 表面改性; 涂层

作者简介: 曹将栋, 男, 1979 年生, 博士, 副教授, 南通航运职业技术学院机电系, 江苏 南通 226010, 电话: 0513-85960874, E-mail: caojd@ntsc.edu.cn